



ELSEVIER

Contents lists available at ScienceDirect

Neurocomputing

journal homepage: www.elsevier.com/locate/neucom

Integration of the saliency-based seed extraction and random walks for image segmentation



Chanchan Qin^a, Guoping Zhang^a, Yicong Zhou^d, Wenbing Tao^{b,c,e,f,*}, Zhiguo Cao^{b,c}

^a College of Physical Science and Technology, Central China Normal University, Wuhan 430079, China

^b School of Automation, Huazhong University of Science and Technology, Wuhan 430074, China

^c National Key Laboratory of Science & Technology on Multi-Spectral Information Processing, Huazhong University of Science and Technology, Wuhan 430074, China

^d Department of Computer and Information Science, University of Macau, Macau 999078, China

^e Hubei Key laboratory of Intelligent Wireless Communication, Wuhan 430074, China

^f State Key Laboratory for Novel Software Technology, Nanjing University, Nanjing, China

ARTICLE INFO

Article history:

Received 26 February 2013

Received in revised form

10 September 2013

Accepted 20 September 2013

Communicated by X. Gao

Available online 23 October 2013

Keywords:

Automatic image segmentation

Superpixels

Saliency estimation

Random walks

ABSTRACT

In this paper, a novel automatic image segmentation method is proposed. To extract the foreground of the image automatically, we combine the region saliency based on entropy rate superpixel (RSBERS) with the affinity propagation clustering algorithm to get seeds in an unsupervised manner, and use random walks method to obtain the segmentation results. The RSBERS first applies entropy rate superpixel segmentation method to split the image into compact, homogeneous and similar-sized regions, and gets the saliency map by applying saliency estimation methods in each superpixel regions. Then, in each saliency region, we apply the affinity propagation clustering to extract the representative pixels and obtain the seeds. A relabeling strategy is presented to ensure the extracted seeds inside the expected object. Additionally, in order to enhance the effects of segmentation, a new feature descriptor is designed using the covariance matrices of coordinates, color and texture information. Experiments on publicly available data sets demonstrate the excellent segmentation performance of our proposed method.

© 2013 Elsevier B.V. All rights reserved.

1. Introduction

According to certain similar criteria of some low-level visual features, such as color, texture, shape etc., image segmentation refers to partition a single image into non-overlapping regions, and then extract the objects of interest under the complex background environment. It has been found, in a wide range of applications, to be not only a fundamental problem but also the key problem in the research of image analysis, pattern recognition [1], computer vision, medical image processing [2], and even image understanding. It is precisely because of its important academic value and great potential for practical application, a lot of research works in this area have been developed in the last 2 decades. According to the fact whether requiring the user's participation in the segmentation process, existing image segmentation methods can be generally divided into automatic and interactive methods.

Automatic approaches do not require any user participation and prior information about the image. Given an image, these

methods can obtain segmentation results automatically. Shi and Malik [3] defined image segmentation as a graph partitioning problem and developed normalized cuts criteria to partition the graph. In [4,5] level set framework is developed for image segmentation, which is based on boundary contours evolution. Mean shift [6] method is still considered as the most important algorithm for color image segmentation. Recently, an unsupervised image segmentation algorithm was presented in [7]. This method modeled each phase using multiple piecewise constants, and minimized the new energy model with graph cuts optimization method. Ugarriza et al. [8] adopted the dynamic region growing and multi-resolution merging technique for automatic natural image segmentation. Browning et al. [5] proposed the ViSTARS neural model which uses motion information to segment objects in response to video inputs from real and virtual environments. Although those approaches can automatically partition image into some separate regions, due to the lack of prior information about the objects in an image, it is hard to provide the ideal segmentation results about real-world natural scene images.

Interactive image segmentation methods incorporate minimal user interactive into the segmentation process. Due to its good segmentation performance, interactive methods have attracted significant attentions in recent years. A representative segmentation method that

* Corresponding author at: School of Automation, Huazhong University of Science and Technology, Wuhan 430074, China. Tel.: +86 27 87540164.

E-mail address: wenbingtao@hust.edu.cn (W. Tao).

belongs to the boundary-based interactive segmentation method has been proposed by Mortensen and Barrett [9]. This method requires the user to control the mouse along the boundary of the object and place several marks, and the Dijkstra's shortest path algorithm is then used to finish the segmentation of the object. Another example of interactive segmentation method is the active contour method [10], which is able to capture salient image contour. In this method, an initial contour is placed near the boundary of the object of interest and the contour is evolved to catch the object boundary.

The third method is seed-based interactive segmentation method. The typical methods are the graph cuts based methods [11–15] and random walks algorithm [16]. The user is asked to provide an initial labeling of some pixels as belonging to the desired object or background (known as seeds), and then the algorithm completes the labeling for all pixels in the image based on the seed clues. Here image segmentation is treated as a graph optimization problem and the image is represented as a weighted graph where each vertex of this graph corresponds to a pixel or region and each edge with weight indicates the similarity relationship between neighbor pixels. Boykov and Jolly [11] proposed the interactive graph cuts method for gray-scale image segmentation method, where the probability distributions of the image foreground and background are described with histograms of gray values, and then the min-cut algorithm is adopted to find the globally optimal segmentation. Similarly in [12] the authors proposed a coarse-to-fine interactive foreground extracted method named Lazy Snapping, where the multiple average color of these seed regions is used to build the distributions of the foreground and background. Rother et al. proposes GrabCut [13] method, where the Gaussian mixture model is used to model the foreground and background and the iterative process between model estimation and parameter learning based on graph cuts is used to optimize the segmentation results until convergence. Tao et al. [17,18] extended the interactive binary segmentation to multiphase image method based on variational model and graph cuts optimization. Hu et al. [19] presented a fast and accurate semiautomatic contour delineation method. It uses a conditional random field graphical model to define the energy minimization function for obtaining an optimal segmentation, and applies a graph partition algorithm to efficiently solve the energy minimization function. The random walks algorithm [16] treats the edge weights as probabilities of a particle at one node traveling to a neighboring node. Given seeds, the probability that a particle at any unlabeled pixel first travels to the foreground or background seeds are used as the basis for image segmentation [16,20].

These interactive methods introduced above can achieve impressively accurate results. However, the manual interactions are

time-consuming and often infeasible in many practical applications. These shortcomings limit the applications of the interactive methods for image segmentation.

The segmentation quality of current interactive tools depends heavily on the seeds extraction. To address the inherent problems of the interactive image segmentation methods, some researchers have been tried to develop full-automatic segmentation approaches by integrating the saliency detection technologies. Firstly the object seeds are extracted by some saliency detection methods, and then one interactive segmentation method is used to finish the final object segmentation. There are many methods to extract saliency regions from an image based on human visual theory [21–31]. Fu et al. [32] put forward an approach named Saliency cuts, which designs a multi-resolution framework to provide the object segmentation automatically. In [33], an iterative self-adaptive framework is developed and the min-cut algorithm is used to segment the salient objects. Cheng et al. [31] automatically initialized GrabCut by binarizing the saliency map, and then iteratively applied GrabCut to improve the segmentation results.

Recently the random walks segmentation has been introduced to interactive image segmentation and shown to have desirable theoretical properties and perform well in many practical applications [16]. Its major advantage is that the solution for random walk energy function is exact and unique minimum. Therefore, this method can likely achieve better performance especially in the presence of weak boundaries and noise. However, due to the fact that it lacks a global feature distribution model, the random walks method is very sensitive to positions and quantities of foreground and background seeds. It is known that the positions of the comprehensive and uniform seeds would lead to accurate segmentation results and reduce or even eliminate the user interactions. However, the inaccurate selection of seeds usually results in inaccurate region labeling results so that more user interactions are required to extract the object of interest accurately. An example of this inherent problem of random walks is shown in Fig. 1, images with the superimposed seeds are shown in the first row, and the corresponding segmentation is displayed in the second row. As shown in columns 1–4 of Fig. 1, we can find that the segmentation results vary significantly from each other although the foreground and background seeds are all accurately marked. Comparatively, the position of comprehensive and uniform seeds position leads to a more pleasant segmentation result as shown in the last column of Fig. 1.

In this paper, we propose an automatic segmentation method using the random walks framework. In order to extract seeds with sufficient and accurate information automatically, this paper proposes an efficient seeds extraction method by integrating the

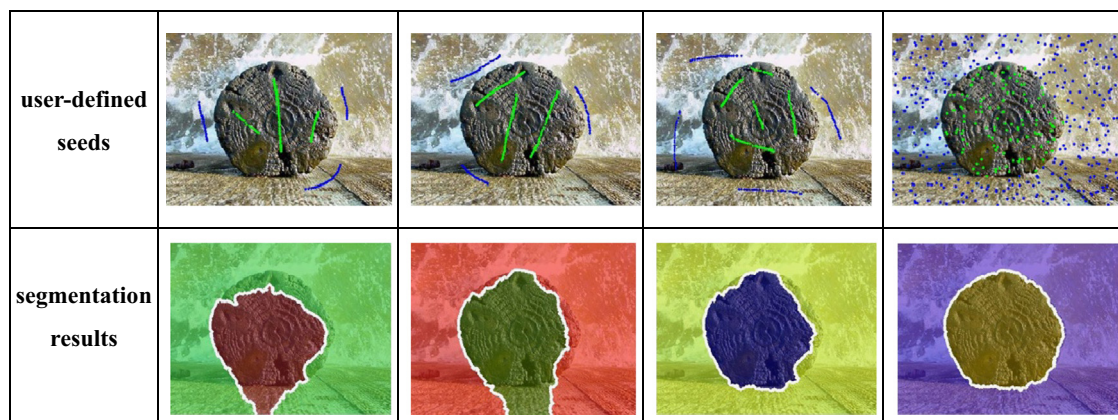


Fig. 1. Dependency on the seeds of random walks algorithm. The first row shows the original images (#0_3_3524 from the saliency object database Free 1000) with superimposed user-specified seeds (green lines (points) for the foreground and blue lines (points) for background) and the second row displays the segmentation results obtained from the corresponding seeds. (For interpretation of the references to color in this figure legend, the reader is referred to the web version of this article.)

entropy rate superpixels [34], saliency estimation and affinity propagation clustering method [35]. We first combine the superpixel segmentation method with the global contrast based saliency estimation approach to obtain the region saliency based on entropy rate superpixel (RSBERS). The entropy rate superpixel segmentation algorithm [34] has the potential to improve the overall segmentation results as well as to reduce computation time. Compared with the traditional global contrast based algorithm, the RSBERS method can avoid the effect of noise and the elements loss by averaging the saliency values in each superpixels region and lead to more accurate saliency map. In each superpixel saliency region, we apply the affinity propagation (AP algorithm) [35] independently to obtain “exemplars”, which are then labeled by a fixed saliency threshold to obtain seeds. Due to the use of the entropy rate superpixel algorithm, we can find that the extracted seeds can cover the foreground and background comprehensively and uniformly. This is extremely helpful to provide sufficient and accurate information for the succeeding random walks segmentation. To make sure the automatically generated seeds are inside the interest object, a seed relabeling strategy is proposed to eliminate the mislabeled seeds.

Moreover, we integrate the texture feature [36–38] with the color information in the proposed algorithm framework for more accurate seeds extraction by RSBERS method and better segmentation performance by random walk algorithm. We use the multi-scale nonlinear structure tensor (MSNST) to describe the texture feature of images [39–42]. We then design a new strong feature descriptor for local pixel neighborhoods by using covariance matrices of low-level features as proposed by [43,44]. The main advantage of using covariance matrices as local descriptors is that they enable efficient fusion of different types of low-features, such as color, texture, coordinates information etc.

The overview of the proposed methods is presented in Fig. 2. Firstly, the proposed features integrating color and texture information are extracted from the original image. Secondly the saliency estimation is produced and the superpixel segmentation is obtained by entropy rate method. And then the two results are combined to get the saliency regions extraction result. Thirdly, the AP clustering algorithm is applied to each superpixel saliency region to discover the representative pixels and the entropy threshold technique is used to obtain the salient seeds which are considered as the seeds for random walk segmentation. Subsequently, the seed relabeling method is used to remove the unreliable seeds to ensure that the seeds are all inside the object. Finally, the random walk is used to get the last segmentation result based on the seeds.

The remainder of this paper is organized as follows: in Section 2, a new feature descriptor is constructed by using covariance matrices of coordinates, color and texture information. Section 3 introduces our automatic image segmentation method in detail. In Section 4, a number of comparison experiments using the real natural scene images are given to demonstrate the superior performance of our proposed method, followed by a brief conclusion in Section 5.

2. Construction of feature descriptor

With regard to the performance of image segmentation, it depends heavily on the accuracy of feature descriptor. In order to improve the ability of feature description, a new strong color–texture feature descriptor for local pixel neighborhoods was constructed in this section by using covariance matrices of coordinates, color and texture information.

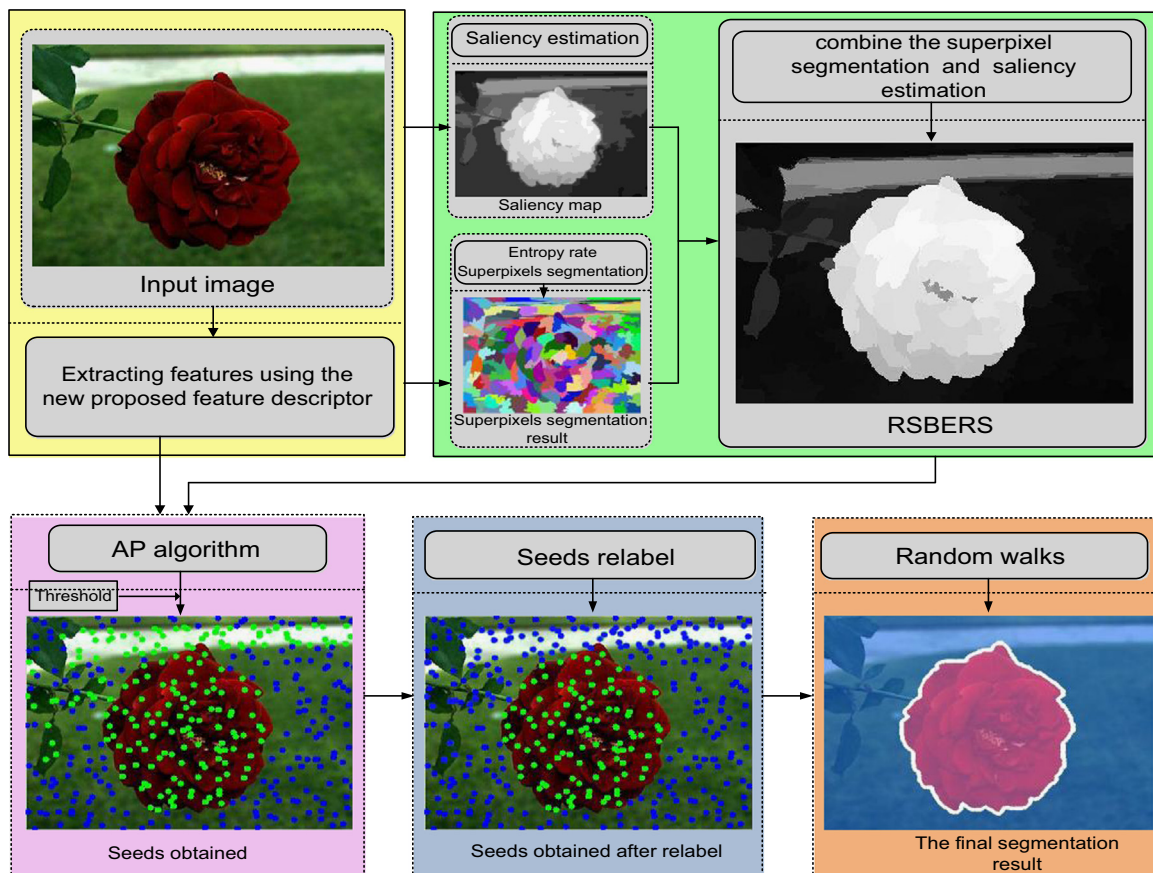


Fig. 2. Flow chart of automatic image segmentation.

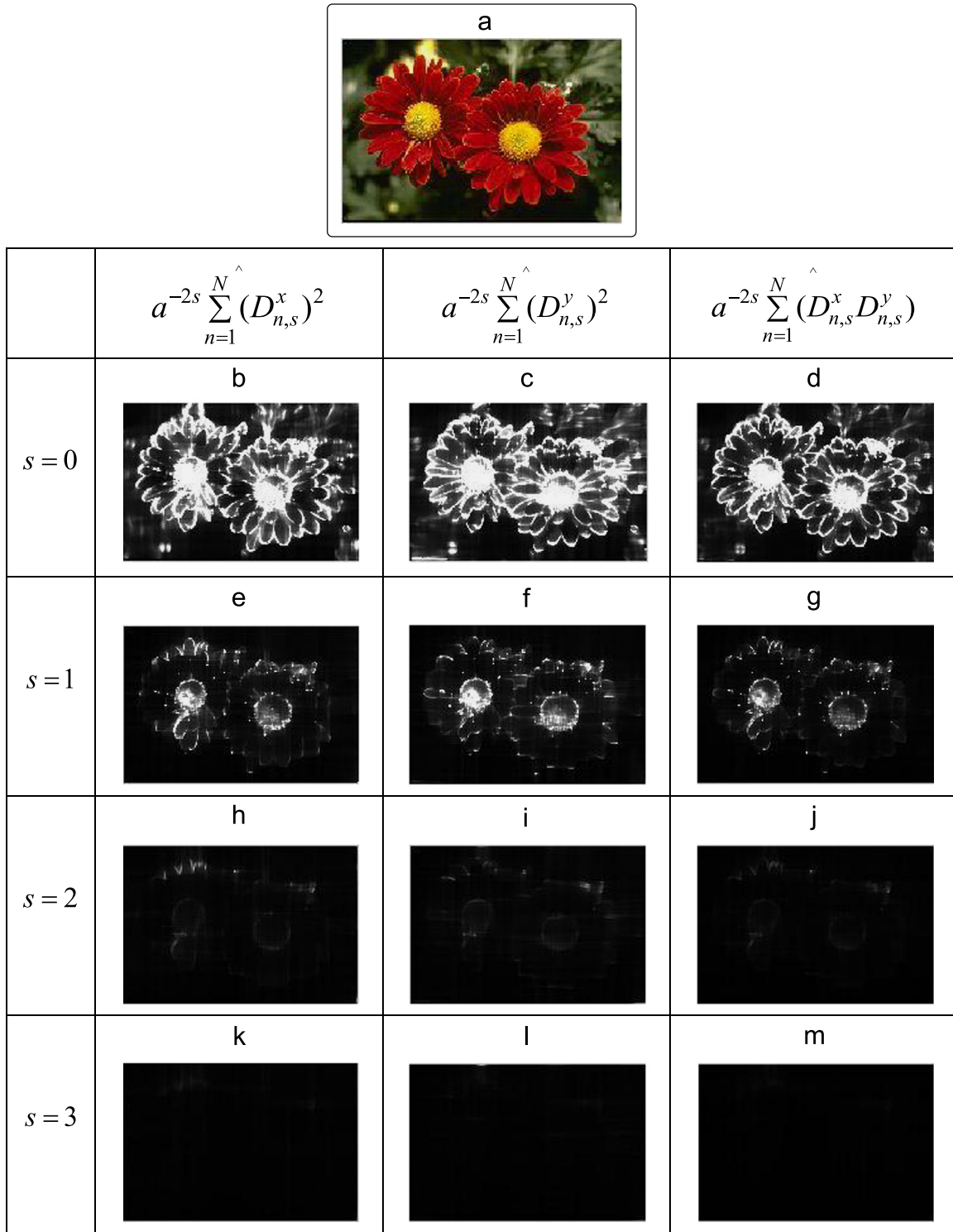


Fig. 3. Multiscale nonlinear structure tensor with four scales: (a) original image (#124084 from the Berkeley segmentation database BSD300); (b)–(d) the first scale of MSNST with $s=0$; (e)–(g) the second scale of MSNST with $s=1$; (h)–(j) the third scale of MSNST with $s=2$; (k)–(m) the fourth scale of MSNST with $s=3$.

Given the image I , we can use the nonorthogonal discrete wavelet to compute multi-scale structure tensor [45]. Let T_s be the s -th scale tensor of MSST, which can be constructed using the tensor product of gradient as

$$T_s = \sum_{n=1}^{N_c} (\nabla(I * \theta_s)_n \nabla(I * \theta_s)_n^T)$$

$$= \alpha^{-2s} \begin{pmatrix} \sum_{n=1}^{N_c} (D_{n,s}^x)^2 & \sum_{n=1}^{N_c} (D_{n,s}^x D_{n,s}^y) \\ \sum_{n=1}^{N_c} (D_{n,s}^x D_{n,s}^y) & \sum_{n=1}^{N_c} (D_{n,s}^y)^2 \end{pmatrix},$$

$$s = 0, 1, \dots, S-1$$

(1)

where S represents the total number of scales in the multi-resolution decomposition, and θ_s is the corresponding convolution

operator in s -th scale. α is the shrinkage coefficient of wavelet. The subscript n denotes the n -th color channel of the image I and N_c is the total number of the color channels. The notations $D_{n,s}^x$ and $D_{n,s}^y$ represent partial derivatives of the n -th color channel of the image in s -th scale. The nonlinear diffusion filtering is adopted to smoothen the noises and enhance the edges simultaneously to obtain MSNST.

For most of the natural image, their texture information is mainly focused on a few scales and the overlage S will include lots of information redundant. Fig. 3(a) shows an image and Fig. 3 (b)–(m) displays the corresponding MSNST of four scales. It can be seen from the figure that the main texture information is mostly concentrated in the first two scales. Consequently, we only use the first two scales, which $s=0$ and $s=1$, in our new feature description.

Since the MSNST matrices set have different feature structures from color and coordinate vector, they cannot be used to construct covariance matrices directly. To address this problem, we first straighten the two-dimensional matrix of MSNST into a one-dimensional row vector. Consider that the matrix of MSNST is symmetric, texture information can be expressed as $(T_s(1,1) T_s(1,2) T_s(2,2))$. Therefore, we use a 11-dimensional feature vector f by integrating the coordinates, texture information, and the Lab color (for Lab, it was shown to be approximately perceptually uniform) for constructing covariance matrices which is defined as

$$f = [xyLabT_0(1,1) T_0(1,2) T_0(2,2) T_1(1,1) T_1(1,2) T_1(2,2)] \quad (2)$$

where x and y are the normalized pixel coordinates, L , a and b are the pixel values of the Lab color space and $T_0(1,1)$, $T_0(1,2)$, $T_0(2,2)$, $T_1(1,1)$, $T_1(1,2)$ and $T_1(2,2)$ are the corresponding first and second scale MSNST. For instance $T_0(1,1) = a^{-2s} \hat{\sum}_{n=1}^{N_c} (D_{n,s}^x)^2$, and the “hat” denotes that corresponding component has been nonlinearly diffused.

Then, we define a fixed neighborhood size $N \times N$ for every pixel and calculate the symmetric 11×11 covariance matrix Σ by

$$\Sigma = \begin{pmatrix} \sigma_{11} & \cdots & \sigma_{1 \ 11} \\ \vdots & \ddots & \vdots \\ \sigma_{11 \ 1} & \cdots & \sigma_{11 \ 11} \end{pmatrix} \quad (3)$$

$$\sigma_{ij} = \frac{1}{N^2 - 1} \sum_{n=1}^{N^2} (f_i^n - \mu_i)(f_j^n - \mu_j) \quad (4)$$

where μ_i is the mean value of the i -th feature f_i . Due to the fact that the covariance matrices are symmetric, we get a 55-dimensional feature vector containing low-level information of local neighborhood for every pixel.

Taking into account the Riemannian structure of the covariance matrices, the distances of two covariance matrices can be measured in manifold space as in [46].

3. Automatic image segmentation method

In this section, an automatic image segmentation method was proposed. Our proposed method consists of three steps. First, we combine the entropy rate superpixel segmentation method and saliency estimate algorithm to obtain region saliency based on entropy rate superpixels (RSBERS) (Section 3.1). Second, seed extraction and relabel scheme are proposed (Section 3.2). Finally, all extracted seeds are regard as priori information integrating interactive random walks methods to obtain segmentation results (Section 3.3). In Fig. 4, we visualize some intermediate states in the process of our automatic seeds extraction method. Fig. 4(a) shows a real natural image (#0_11_11987 from the saliency object database Free 1000 [29]). The entropy rate superpixel segmentation results with random color are displayed in Fig. 4(b). The results of REBERS and the boundaries of superpixel segmentation with superimposed representative pixels (boundaries with blue line and representative pixels with red points) are shown in Fig. 4 (c) and (d). The seeds obtained before and after relabeling scheme are shown in Fig. 4(e) and (g), respectively. Finally, the segmentation results before and after seeds relabel scheme are shown in Fig. 4(f) and (h).

3.1. Region saliency based on entropy rate superpixel (RSBERS)

Recently many visual saliency models and attention models have been presented [21–31], which lead to a number of application, such as object recognition [47–49], image segmentation [50],

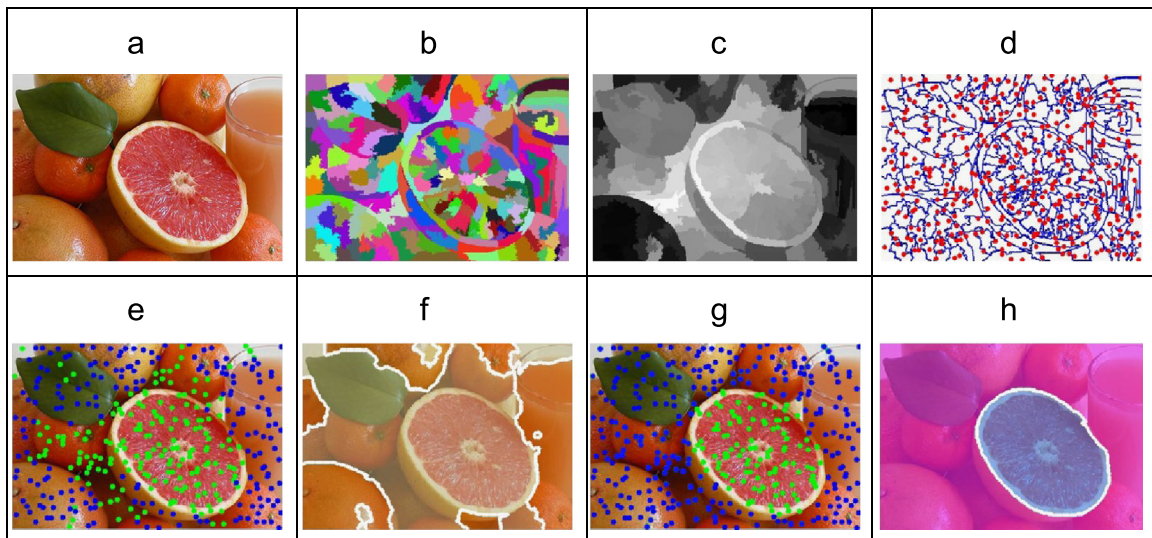


Fig. 4. The detailed performance of automatic seeds extraction. The image comes from the saliency object database Free 1000 [29]: (a) original image (#0_11_11987); (b) superpixel segmentation result with randomly color (image contain 200 superpixels) by entropy rate superpixel method; (c) the result of region saliency based on entropy rate superpixel (RSBERS); (d) the boundaries of superpixel segmentation with superimposed representative pixels (boundaries with blue line and representative pixels with red points); (e) seeds obtained before relabel scheme (green points for foreground marker and blue points for background marker); (f) segmentation result of our approach without relabel scheme; (g) seeds obtained after relabel scheme; (h) segmentation result of our approach with relabel scheme. (For interpretation of the references to color in this figure legend, the reader is referred to the web version of this article.)

image retrieval [51] etc. Depending on the extent of the context where the contrast is computed, previous methods can be categorized as local methods [22–27] or global methods [28–31]. Local contrast based methods compute various contrast measures in a local neighborhood of the pixel/patch. Such methods tend to produce higher saliency values near edges. While global contrast based methods, which use the entire image to compute the saliency of individual pixels/patches, have the advantage of highlight the entire objects uniformly. Consider that we focus on the whole object in our image segmentation method, this paper adopt the global contrast based methods.

Global contrast based saliency estimation methods have achieved success in their own aspects, but still have certain limitations. Typically, as shown in Fig. 5(c)–(e), the salient object can be found well, but there may contain plenty of noises and sometimes elements lost. The “inaccurate” problem is observed in all pixel-based methods [28–31]. It is alleviated in region-based methods of RC in [31], but the RC methods still have difficulties of extracting the accurate boundary as shown in Fig. 5. These disadvantages may lead to mislabeled seeds and eventually imprecise segmentation results. To tackle this problem, we put forward the region saliency based on entropy rate superpixel (RSBERS) method, which combines the entropy rate superpixel segmentation [34] and saliency estimate approaches. First, we use entropy rate superpixel segmentation method to group pixels into perceptually meaningful atomic regions (shown in Fig. 4(b)). Liu [34] studied the superpixel segmentation as a clustering problem and presented a new clustering objective function including two terms. The entropy rate encourages division of images on perceptual boundaries and favors superpixels overlapping with only a single object, whereas the balancing term reduces the number of unbalanced superpixels and hence preserves object boundaries. These all favors accurate saliency estimate. Then, in each superpixels region we average the pixels saliency value to

obtain the region saliency, which makes sure that each superpixels saliency region shares the same saliency value. In this paper, we integrate three different saliency estimate methods: HC [31], RC [31] and SF [30].

The results of RSBERS are shown in Fig. 4(c) and the last column of Fig. 5. It is observed that the RSBERS method can guarantee the perceptual boundaries and share the same saliency value in each superpixel region. Moreover, the use of superpixels segmentation algorithm makes seeds extracted in following step cover the foreground and background comprehensively and uniformly. It is straightforward benefit to the segmentation results.

3.2. Seed extraction and relabel scheme

The region saliency based on entropy rate superpixel (RSBERS) step of Section 3.1 provides a relatively satisfied saliency map. In order to obtain comprehensively and uniformly seeds distribution automatically, we then apply the affinity propagation clustering algorithm (AP) [35] in each of these superpixel saliency regions to discover representative pixels, which we call “exemplars”, from an image.

AP algorithm was recently proposed by Dueck and Frey. It has been proved to be more effective than the classical clustering methods, such as k -means, k -centers, the expectation maximization (EM), spectral clustering [52–55] etc. AP algorithm considers all data points of randomly selected subset as candidate centers. Using this method, many of the poor solutions caused by unlucky initializations can be avoided. In addition, the number of identified exemplars (number of clusters) in AP algorithm is not required to pre-defined and influenced by the values of the input preferences. Most important, unlike classical clustering method, the exemplar for each cluster may not have a real-world interpretation (for example, in k -means, the exemplar is the mean of the data points in each cluster). The exemplar

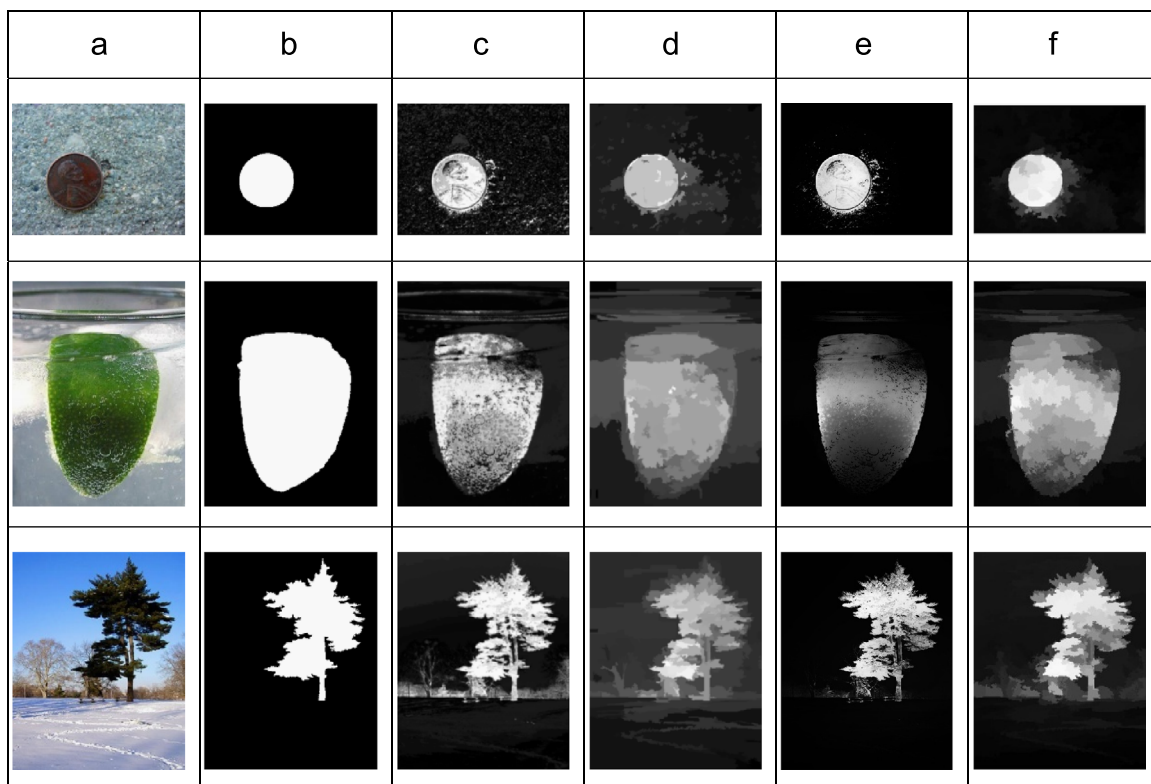


Fig. 5. Saliency maps on three example images. The images come from the saliency object database Free 1000 [29]: (a) input images; (b) ground truth salient object masks; (c) results from the HC method proposed in [31]; (d) results from the RC method proposed in [31]; (e) results from the SF method proposed in [30]; (f) results from our RSBERS method.

obtained by AP algorithm is one of the data points. It is important in our method, because we hope that the property of the data points can be best expression by the exemplar, which must belong to the data points.

Fig. 4(d) shows the boundaries of superpixel segmentation with superimposed representative pixels (boundaries with blue line and representative pixels with red points). The use of affinity propagation clustering algorithm [35] not only decreases the redundancy information and reduces the following complexity of calculation and space, but also provides sufficient and accurate information, which is beneficial to obtain excellent segmentation results. Note that, in order to further improve the speed of the whole algorithm, we first perform a down-sampling processing on each superpixel region.

Following, the representative pixels are labeled by using a threshold (the pixels with higher saliency value than the threshold are assigned label 1, and with lower saliency value than the threshold are assigned label 0). The entropic thresholding technique [56] is used to obtain an optimal threshold that is adaptive to the image contents. Fig. 4(e) shows the seeds, which comprehensively and uniformly covers the object and background regions, obtained by our method (green points for foreground marker and blue points for background marker). As we can see from the Fig. 4(e), the extraction seeds are sometimes with wrong labels. Due to that the object segmentation results are dominated by the reliability of extraction seeds label in the automatic object segmentation, as well as in the interactive random walks approach. The error labeling information will greatly affect the corresponding segmentation accuracy. As can be seen from Fig. 4(f), the image is actually error-segmented. To address this problem, we propose a seeds relabeling method, which can reduce the mislabeled seeds.

Our seed relabeling method is inspired from the iterative energy minimization method in [13], which estimate the probability density distribution of the background and foreground Gaussian mixture models, and then using iteratively refines the parameters using a combination of graph cuts and EM-like estimation until reach a maximum number of iterations or convergence criteria.

In this paper, we treat the seed relabeling task as that of estimating a set of binary variables $X = \{x_i \in \{0, 1\} : i = 1, 2, \dots, N\}$, each indicating whether the corresponding seed belongs to foreground or background. Similar to [13], K components Gaussian Mixture Models (GMMs) for our obtained object seeds and background seeds represented by $G^o(x_i; \pi^o, \mu^o, \Sigma^o)$ and $G^b(x_i; \pi^b, \mu^b, \Sigma^b)$

respectively. To obtain the accurate labels of the seeds, we can construct a corresponding energy function and minimize it. Follow the definition of traditional graph cuts [14], the energy function can be designed as $E = U + \lambda V$ where U and V denote the data term and smoothness term respectively, and the balance factor of these two terms are weighted by $\lambda \geq 0$. To minimize the energy function E we construct a weighted graph to solve the minimizing cuts problem and update the statistical parameters of weights π means μ and covariances Σ iteratively.

After completing the processes of relabeling, we can obtain relatively satisfied labels of all seeds and accurate segmentation results (as shown in Fig. 4(g) and (h)). It can be found that iterative relabeling scheme can reduce mislabeled seeds. In addition, we should notice that the method only require minimal time, because the number of seeds is small (about 200) when compared with the total number of pixels of the image. We set the number of iterations as 4, which has been demonstrated to be enough for most of the experiments. (More verification experiments are given in Figs. 7–9.)

3.3. Integrating automatic seeds extraction and random walks segmentation

In the random walks method, the edge weights are treated as probabilities of a particle at one node traveling to a neighboring node. The edge weights function is formulate as

$$w_{ij} = \exp(-\beta(g_i - g_j)^2) \quad (5)$$

where g_i indicates the image feature (in this paper, feature descriptor introduced in Section 2) at pixel i . The value of β represents the only free parameter in this algorithm. Given a small number of seeds, segmentation begins with labeling a pixel in such a way that the pixel is assigned a label with the greatest probability if a random walker starting its walk at this pixel first reaches a seed with that label. It is essentially an approach that minimizes Dirichlet energy with boundary conditions.

Our studies show that the performance of the random walks algorithm is sensitive to the distribution of the seeds. This is mainly because the random walks algorithm lacks a global feature distribution model. Therefore, even in the cases that the foreground and background seeds are accurately marked as internal and external, the random walks algorithm may require more carefully user interaction to obtain an accurate segmentation.

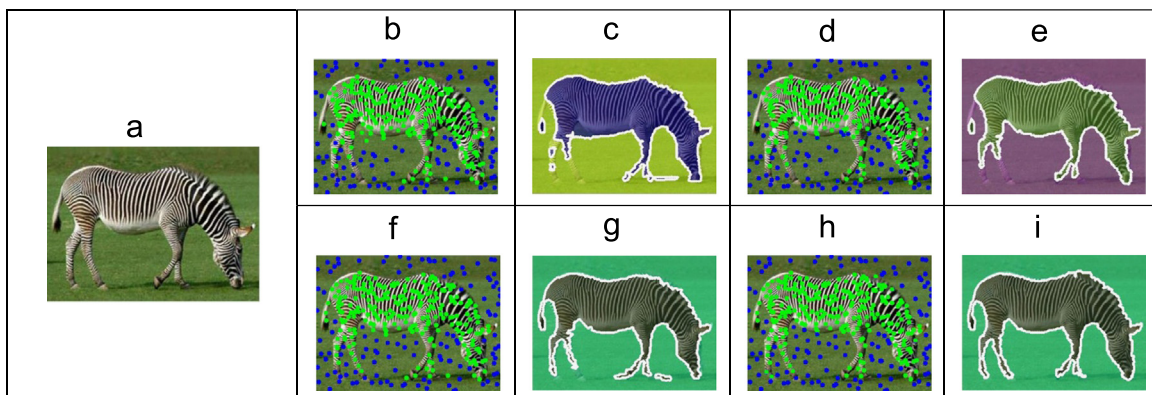


Fig. 6. Testing the performance of the feature descriptor: (a) input images; (b) original images with superimposed seeds (green points for foreground marker and blue points for background marker), which obtained without using relabeling scheme (using color information only); (c) segmentation results before relabeling scheme (using color information only); (d) original images with superimposed seeds after relabeling scheme (using color information only); (e) final segmentation results (using color information only); (f) original images with superimposed seeds before relabeling scheme (using our proposed feature descriptor); (g) segmentation results before relabeling scheme (using our proposed feature descriptor); (h) original images with superimposed seeds after relabeling scheme (using our proposed feature descriptor); (i) final segmentation results (using our proposed feature descriptor). (For interpretation of the references to color in this figure legend, the reader is referred to the web version of this article.)

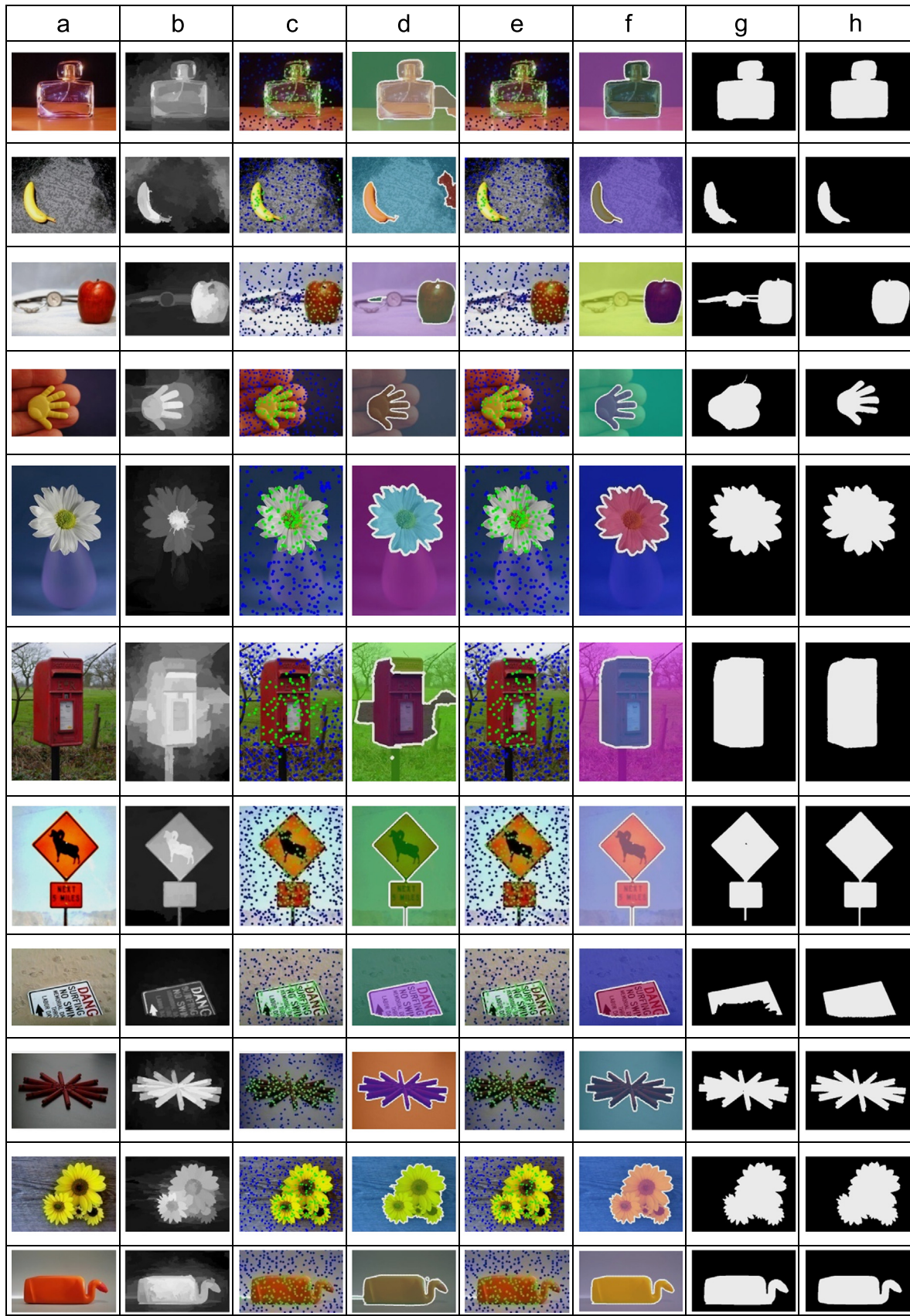


Fig. 7. Comparison of segmentation results for images which contain some saliency objects. The images come from the saliency object database Free 1000 [29]: (a) original images; (b) results of our region saliency based on entropy rate superpixel (RSBERS); (c) original images with superimposed seeds (green points for foreground marker and blue points for background marker), which obtained without using relabel scheme; (d) segmentation results without seeds relabel scheme; (e) seeds obtained after relabeling; (f) final segmentation results; (g) segmentation results of Saliency cut [31]; (h) ground truths [29]. (For interpretation of the references to color in this figure legend, the reader is referred to the web version of this article.)



Fig. 8. Testing of segmentation results on natural images. The images come from the Berkeley segmentation database BSD300 [57]: (a) original images; (b) original images with superimposed seeds (green points for foreground marker and blue points for background marker), which obtained without using relabeled scheme; (c) segmentation results without seeds relabeled scheme; (d) seeds obtained after relabeled scheme; (e) final segmentation results; (f) segmentation results of Saliency cut [31]. (For interpretation of the references to color in this figure legend, the reader is referred to the web version of this article.)

As discussed in Section 1, unreliable seeds usually result in region lost or false regions. However, if the seeds cover the foreground and background comprehensively and uniformly, the segmentation results would be greatly improved. The seeds distribution, provided by our automatic seeds extraction method introduced in the above section are passed as an initialization to random walks segmentation method. Our proposed method can provide sufficient and accurate information, and favors excellent segmentation results as shown in Fig. 4(h).

4. Experiments

In our experiments, we provide a number of real natural scene images for comparison, and these images are all from Berkeley segmentation database BSD300 [57] and the saliency object database Free 1000 [29]. Additionally, to visualize the segmentation results more intuitively, we color the foreground and background with a different translucent color randomly.

Input image	classical random walks			Our method
 #4_144_144868	  (0.9008/0.0714/ 0.4675/4.4152)	  (0.9825/0.0168/ 0.1273/1.9451)	  (0.9912/0.0087/ 0.0761/0.7815)	  (0.9912/0.0087/ 0.0754/0.7518)
 #0_12_12435	  (0.8072/0.1675/ 0.8996/19.8705)	  (0.9708/0.0288/ 0.2114/2.9546)	  (0.9886/0.0111/ 0.0902/0.9695)	  (0.9928/0.0071/ 0.0636/0.5487)
 #0_3_3524	  (0.6630/0.2734/ 1.3514/20.4507)	  (0.9093/0.0819/ 0.4863/7.9517)	  (0.9826/0.0173/ 0.1392/1.1615)	  (0.9828/0.0171/ 0.1404/1.1619)

Fig. 9. The qualitative and quantitative comparisons of for classical random walks method [16] with different user-specified seeds and our proposed method. The images come from the saliency object database Free 1000 [29].

4.1. Parameter settings

In this section, in order to demonstrate the performance of image segmentation when using our proposed automatic method, in the following sections, we chose the interactive random walks method [16] and the Saliency cut method [31] for comparison.

The main parameter settings of the above two methods should be given in advance for a reasonable comparison. The Saliency cut method has two parameters to be appropriately predefined. Just like the authors suggest, we set spatial weighting and the number of iterations as 0.4 and 4 respectively. For the random walks algorithm, the free parameter is fixed as 90. Here, notice that the

sources codes of the two methods can be downloaded from the author's websites [58,59].

Additionally, some parameters of our proposed method also appropriately predefined. Since the main texture information is mostly concentrated in the first two scales, the scale number S in formula (1) is set as 2. The local window size N is set to 15 in formula (4). The number of superpixels is set to 200 in all experiments. When implementing the AP algorithm, we set the input preferences to be the median of the input similarities in order to result in a moderate number of clusters. Please refer to Table 1 for more details about parameters setting.

Table 1
Parameters setting of all used methods.

Feature descriptor	
Number of scales S	2
Total number of the channels N_c	3
Basis of wavelet α	2
Local window size N	15
Entropy rate superpixels segmentation	
Balancing parameter	0.5
Gaussian kernel bandwidth	5.0
Number of superpixels	200
Saliency estimate	
RC	
Spatial weighting	0.4
SF	
Scaling factor	6
Control parameter	0.25
Random walks image segmentation	
Free parameter	90
Seeds relabel scheme	
K	5
Number of iterations	4

4.2. Comparison and analysis experiments

In Fig. 6, we test the performance of our proposed feature descriptor. Fig. 6(a) presents a natural image, which contains rich texture information. Through the compared results presented in Fig. 6(b)–(i), we can find that our proposed feature descriptor has more powerful discriminating ability. Using this new feature descriptor, we can not only extract sufficient and accurate seeds position, but can also obtain superior segmentation results.

We will test the comprehensive segmentation performance of our proposed approach qualitatively and quantitatively in the following experiments. First, we use some testing images from the salient object database Free 1000 [29]. Fig. 7(a) displays all the images we used, including #1_47_47781, #2_78_78470, #1_47_47334, #3_95_95684, #1_58_58944, #0_0_272, #1_47_47779, #0_0_77, #0_0_284, #0_5_5887 and #1_66_66254. Moreover, another automatic image segmentation method (Saliency cut) [31] are chosen for comparison. The results of our region saliency based on entropy superpixels (RSBERS) are displayed in the second column of Fig. 7. The third column of Fig. 7 shows the seeds obtained before relabel scheme. Although these seeds can cover the object and background comprehensively and uniformly, there still exist lots of mislabeled seeds, especially for the examples in rows 1, 2 and 6 of Fig. 7. Integrating the relabeling scheme, we can get an ideal seeds distribution as shown in the fifth column. The corresponding/ segmentation results based on the seeds before and after the relabel scheme are shown in the fourth and sixth columns respectively. The experiments demonstrate that our proposed seeds relabeling strategy can effectively reduce the mislabeled seeds and is helpful for improving the performance of segmentation. The seventh column shows the segmentation results of Saliency cut [31]. Finally, the ground truths are shown in the eighth column. From the comparisons of segmentation results, we can find that the method of Saliency cut can obtain accurate segmentation results in most images, but there still exist

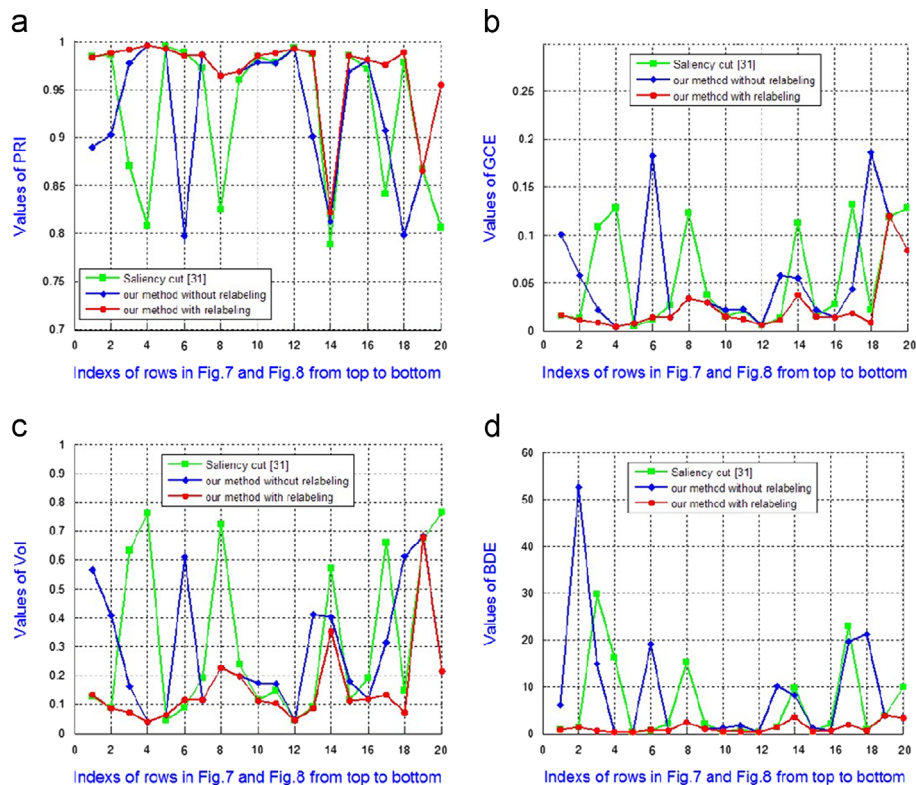


Fig. 10. The quantitative comparisons of the PRI, GCE, Vol and BDE for our approach without relabeling, our method with relabeling and Saliency cut method [31] with the indexes of rows (from top to bottom in Figs. 7 and 8) as the horizontal axis.

error-segmentations in some images, especially for the results in rows 3, 4 and 8 in Fig. 7. Most of the segmentation results of our approach are superior to the method of Saliency cut, and are closest to the actual saliency objects (ground truths).

To further verify the performance of our proposed segmentation method, some testing images from the Berkeley segmentation database BSD300 [57] are shown in Fig. 8(a), including #3096, #12003, #196073, #124084, #135069, #253036, #41004, #12074 and #35070. We also choose the Saliency cut method [31] for comparison. Actually, representative images with the different amount of feature information are selected in our experiments. First, the images of starfish and coral contain rich texture information. Second, there are also multiple objects, such as the image in the sixth row. From the comparisons of segmentation results, we can draw the conclusion that our approach has better performance. For example, the plane and the bird are images of one object with simple background, and we can find the object accurately even without relabel scheme. For the images of flowers, starfish, deer, elephant and coral, we can obtain satisfied segmentation results after the relabel scheme. As for the snake image presented in the third row of Fig. 8 is a challenging case, and an unsatisfied result was obtained. This is because the target and background have little differences in this image, which affects the seeds location and then the segmentation result.

We further test the segmentation results of our proposed automatic image segmentation method when compared with the classical interactive random walks segmentation algorithm [16]. The testing images are also from the salient object database Free 1000 [29]. From the comparison experiments, we can find that manual interactions may cause inaccurate or even incorrect segmentation results and involve more interactions to obtain satisfied results (as shown in the middle columns of Fig. 9). The images with superimposed seeds, which obtained by our proposed automatic seeds extraction method and the corresponding segmentation results, are displayed in the last column of Fig. 9. The comparison of segmentation results demonstrate the same conclusions as that of Figs. 7 and 8, which verify that our approach can obtain comprehensively and uniformly seeds position automatically and thus excellent segmentation results. Considering that the proposed method is an automatic segmentation method, does not require any user interaction, and is more promising in the practical application.

4.3. Quantitative comparisons and running time

The quantitative comparisons are also important for objectively evaluating the performance of our proposed methods. We choose the four state-of-the-art performance measures simultaneously for

Table 2

Average performance for the experiments of Figs. 7 and 8 (bold indicates best of all the algorithms).

Methods	PRI	GCE	Vol	BDE
Saliency cut [31]	0.9287	0.0539	0.3215	6.0241
Our method without relabeling	0.9307	0.0541	0.2856	8.3813
Our method with relabeling	0.9694	0.0238	0.1535	1.2063

Table 3

Average running time for all the method we used on the Berkeley segmentation database BSD300 [57].

Method	Construct feature descriptor	Entropy rate superpixels	Saliency estimate	Affinity propagation clustering	Random walks algorithm	Seeds relabel	Total cost
Average cost	1.37s	2.82s	0.76s	4.73s	1.57s	0.62s	13.14s

quantitative evaluation. The performance measures contain probabilistic rand index (PRI) [60], variation of information (Vol) [61], global consistency error (GCE) [57] and boundary displacement error (BDE) [62]. Meanwhile, we should notice that the value of PRI and GCE range from 0 to 1, the value of Vol and BDE range from 0 to ∞ . The larger of PRI, the closer of the segmentation result to the ground truths. The smaller of Vol, GCE and BDE, the closer of the segmentation result to the ground truths. The sources codes of the standard image segmentation indices (PRI, Vol, GCE and BDE) can be downloaded from the websites [63].

Fig. 10 shows the quantitative comparisons of the PRI, Vol, GCE and BDE for the three compared approaches with the indexes of rows (from top to bottom in Figs. 7 and 8) as the horizontal axis. To analyze the four charts of Fig. 10, we can observe that the values of the four performance measures for our approach with relabel scheme are almost all better than the Saliency cut method and our method without relabel scheme, but they are slightly worse than the Saliency cut approach for the fifth and sixth images of Fig. 7 and the eighth image of Fig. 8. In addition, we can further demonstrate the superior accuracies of our method with relabeling by using the mean value of the four performance measures in Table 2. Taking into account the mean (PRI, GCE, Vol, BDE) values, which are (0.9307, 0.0541, 0.2856, 8.3813), (0.9694, 0.0238, 0.1535, 1.2063) and (0.9287, 0.0539, 0.3215, 6.0241) for our method without relabel scheme, our method with relabel scheme and Saliency cut method respectively. These statistics indicate that our approach with relabeling can achieve the highest accuracies in the statistical sense when compared with the other two methods. Additionally, the quantitative comparisons of (PRI, Vol, GCE, BDE) values marked in Fig. 9 also verify that our approach can perform exactly similar as the classical interactive segmentation method, which involve very sufficient user interactions.

The average running time of the proposed automatic segmentation algorithm framework on Berkeley segmentation database BSD300 (481×321 pixels) are reported in Table 3. Including feature descriptor construction, entropy rate superpixels, saliency estimate, affinity propagation clustering, seeds relabel scheme, random walks algorithm and the total cost of the framework. All these experiments are performed on a notebook which is equipped with a 2.40 GHz Intel(R) Core(TM) i3 CPU and 4 GB RAM. The whole system is implemented in MATLAB using OPENCV 1.0 library. Some of the most time consuming operations were implemented in C++ and interfaced with MATLAB through mex-files. Some popular implementations were used the online available C++ or MATLAB code, such as entropy rate superpixel segmentation, affinity propagation etc.

5. Conclusion

In this paper, an automatic image segmentation approach is proposed by combining interactive random walks method with an automated seeds extraction method. We first put forward the region saliency based on entropy rate superpixel (RSBERS), which integrates the entropy rate superpixel segmentation method and saliency estimate approach. It can obtain superior saliency estimate results and improve the accuracy of seeds distribution. Then, we apply the powerful the affinity propagation clustering

algorithm to each superpixels region to get representative pixels, which are then labeled by a fixed threshold to obtain seeds. Meanwhile, a seeds relabeling method is presented and can be used to reduce the mislabeled seeds. Finally, we provide comprehensively and uniformly seeds position automatically, which is important to the following random walks segmentation algorithm. In addition, to improve the powerful feature discriminating ability, a new feature descriptor is designed by integrating coordinates, color and texture information. At last, the comprehensive qualitative and quantitative experiments demonstrate that our proposed method can obtain satisfactory segmentation results. As a future work, we would like to investigate saliency detection algorithms to handle cluttered and textured background and study more powerful feature descriptor to acquire the more reliable and efficient segmentation results.

Acknowledgments

This research has been supported by the National Natural Science Foundation of China under Grants 61073093, 61371140, 61273279 and in part by Grants 2012TS067, 2011-715-5, 51301030401 and 9140A01060111JW0505, by the Macau Science and Technology Development Fund under Grant 017/2012/A1 and by the Research Committee at University of Macau under Grants MYRG113(Y1-L3)-FST12-ZYC and MRG001/ZYC/2013/FST. The authors would like to thank the anonymous reviewers for their valuable comments.

References

- [1] Y. Yue, Q. Shi, G. Hu, J.A. Wang, A composed statistical pattern recognition and geosciences analysis approach for segmentation-based remotely sensed imagery classification, in: Proceedings of the IEEE International Conference on Geoinformatics, 2011, pp. 1–6.
- [2] Z. Tu, X. Bai, Auto-context and its application to high-level vision tasks and 3D brain image segmentation, *IEEE Trans. Pattern Anal. Mach. Intell.* 32 (2010) 1744–1757.
- [3] J. Shi, J. Malik, Normalized cuts and image segmentation, *IEEE Trans. Pattern Anal. Mach. Intell.* 22 (2000) 888–905.
- [4] N. Paragios, S. Osher, *Geometric Level Set Methods in Imaging, Vision, and Graphics*, Springer, Verlag, 2003.
- [5] A. Browning, S. Grossberg, M. Mingolla, Cortical dynamics of navigation and steering in natural scenes: motion-based object segmentation, heading, and obstacle avoidance, *Neural Networks* 22 (2009) 1383–1398.
- [6] D. Comaniciu, P. Meer, Mean shift: a robust approach toward feature space analysis, *IEEE Trans. Pattern Anal. Mach. Intell.* 24 (5) (2002) 603–619.
- [7] L. Liu, W. Tao, Image segmentation by iterative optimization of multiphase multiple piecewise constant model and Four-Color relabeling, *Pattern Recognition* 44 (2011) 2819–2833.
- [8] L.G. Ugarriza, E. Saber, S.R. Vantaram, V. Amuso, M. Shaw, R. Bhaskar, Automatic image segmentation by dynamic region growth and multiresolution merging, *IEEE Trans. Image Process.* 18 (2009) 2275–2288.
- [9] E.N. Mortensen, W.A. Barrett, Interactive segmentation with intelligent scissors, *Graphical Models Image Process.* 60 (1998) 349–384.
- [10] M. Kass, A. Witkin, D. Terzopoulos, Snakes: active contour models, *Int. J. Comput. Vision* 1 (1988) 321–331.
- [11] Y.Y. Boykov, M.-P. Jolly, Interactive graph cuts for optimal boundary and region segmentation of objects in N-D images, in: Proceedings of the ICCV, 2001.
- [12] Y. Li, J. Sun, C.-K. Tang, H.-Y. Shum, Lazy snapping, *ACM Trans. Graphics (ToG)* 23 (2004) 303–308.
- [13] C. Rother, V. Kolmogorov, A. Blake, Grabcut: interactive foreground extraction using iterated graph cuts, *ACM Trans. on Graphics (ToG)* 24 (3) (2004) 309–314.
- [14] Y. Boykov, V. Kolmogorov, An experimental comparison of min-cut/max-flow algorithms for energy minimization in vision, *IEEE Trans. Pattern Anal. Mach. Intell.* 26 (2004) 1124–1137.
- [15] Y. Boykov, G. Funka-Lea, Graph cuts and efficient N-D image segmentation, *Int. J. Comput. Vision* 70 (2006) 109–131.
- [16] L. Grady, Random walks for image segmentation, *IEEE Trans. Pattern Anal. Mach. Intell.* 28 (2006) 1768–1783.
- [17] W. Tao, F. Chang, L. Liu, H. Jin, T. Wang, Interactively multiphase image segmentation based on variational formulation and graph cuts, *Pattern Recognition* 43 (2010) 3208–3218.
- [18] W. Tao, Iterative narrow band based graph cuts optimization for geodesic active contours with region forces (GACWRF), *IEEE Trans. Image Process.* 21 (2012) 284–296.
- [19] Y.-C. Hu, M.D. Grossberg, A. Wu, N. Riaz, C. Perez, G.S. Mageras, Interactive semiautomatic contour delineation using statistical conditional random fields framework, *Med. Phys.* 39 (2012) 4547–4558.
- [20] L. Grady, G. Funka-Lea, Multi-label image segmentation for medical applications based on graph-theoretic electrical potentials, *Computer Vision and Mathematical Methods in Medical and Biomedical Image Analysis*, Springer, Berlin/Heidelberg (2004) 230–245.
- [21] N.C. Foley, S. Grossberg, E. Mingolla, Neural dynamics of object-based multifocal visual spatial attention and priming: object cueing, useful-field-of-view, and crowding, *Cognitive Psychol.* 65 (2012) 77–117.
- [22] L. Itti, C. Koch, E. Niebur, A model of saliency-based visual attention for rapid scene analysis, *IEEE Trans. Pattern Anal. Mach. Intell.* 20 (1998) 1254–1259.
- [23] Y. Ma, H. Zhang, Contrast-based image attention analysis by using fuzzy growing, in: Proceedings of the Eleventh ACM International Conference on Multimedia, 2003, pp. 374–381.
- [24] X. Hou, L. Zhang, Saliency detection: a spectral residual approach, in: Proceedings of the IEEE Conference on Computer Vision and Pattern Recognition, 2007, pp. 1–8.
- [25] R. Achanta, F. Estrada, P. Wils, S. Süsstrunk, Salient region detection and segmentation, *International Conference on Computer Vision Systems (ICVS '08)*, Lecture Notes in Computer Science, Springer 5008 (2008) 66–75.
- [26] T. Liu, Z. Yuan, J. Sun, J. Wang, N. Zheng, X. Tang, H.-Y. Shum, Learning to detect a salient object, *IEEE Trans. Pattern Anal. Mach. Intell.* 33 (2011) 353–367.
- [27] S. Goferman, L. Zelnik-Manor, A. Tal, Context-aware saliency detection, *IEEE Trans. Pattern Anal. Mach. Intell.* 34 (2012) 1915–1926.
- [28] Y. Zhai, M. Shah, Visual attention detection in video sequences using spatiotemporal cues, in: Proceedings of the 14th Annual ACM International Conference on Multimedia, 2006, pp. 815–824.
- [29] R. Achanta, S. Hemami, F. Estrada, S. Süsstrunk, Frequency-tuned salient region detection, in: Proceedings of the IEEE Conference on Computer Vision and Pattern Recognition, 2009, pp. 1597–1604.
- [30] F. Perazzi, P. Krahenbuhl, Y. Pritch, A. Hornung, Saliency filters: Contrast based filtering for salient region detection, in: Proceedings of the IEEE Conference on Computer Vision and Pattern Recognition, 2012, pp. 733–740.
- [31] M. Cheng, G. Zhang, N.J. Mitra, X. Huang, S. Hu, Global contrast based salient region detection, in: Proceedings of the IEEE Conference on Computer Vision and Pattern Recognition, 2011, pp. 409–416.
- [32] Y. Fu, J. Cheng, Z. Li, H. Lu, Saliency cuts: an automatic approach to object segmentation, in: Proceedings of the 19th International Conference on Pattern Recognition, 2008, pp. 1–4.
- [33] C. Jung, B. Kim, C. Kim, Automatic segmentation of salient objects using iterative reversible graph cut, in: Proceedings of the IEEE International Conference on Multimedia and Expo (ICME), 2010, pp. 590–595.
- [34] M. Liu, O. Tuzel, S. Ramalingam, R. Chellappa, Entropy rate superpixel segmentation, in: Proceedings of the IEEE Conference on Computer Vision and Pattern Recognition, 2011, pp. 2097–2104.
- [35] B.J. Frey, D. Dueck, Clustering by passing messages between data points, *Science* 315 (2007) 972–976.
- [36] A. Materka, M. Strzelecki, Texture analysis methods—a review, COST B11 Report, Technical University of Lodz, Institute of Electronics, Brussels, 1998, pp. 9–11.
- [37] T. Randen, J.H. Husoy, Filtering for texture classification: a comparative study, *IEEE Trans. Pattern Anal. Mach. Intell.* 21 (1999) 291–310.
- [38] B.S. Manjunath, W. Ma, Texture features for browsing and retrieval of image data, *IEEE Trans. Pattern Anal. Mach. Intell.* 18 (1996) 837–842.
- [39] P. Pudil, J. Novotná, J. Kittler, Floating search methods in feature selection, *Pattern Recognition Lett.* 15 (1994) 1119–1125.
- [40] C. Reyes-Aldasoro, A. Bhalerao, The Bhattacharyya space for feature selection and its application to texture segmentation, *Pattern Recognition* 39 (2006) 812–826.
- [41] M. Wall, A. Rechtsteiner, L. Rocha, Singular value decomposition and principal component analysis, *A Practical Approach to Microarray Data Analysis*, 91–109.
- [42] S. Han, W. Tao, D. Wang, X. Tai, X. Wu, Image segmentation based on GrabCut framework integrating multiscale nonlinear structure tensor, *IEEE Trans. Image Process.* 18 (2009) 2289–2302.
- [43] F. Porikli, O. Tuzel, P. Meer, Covariance tracking using model update based on lie algebra, in: Proceedings of the IEEE Computer Society Conference on Computer Vision and Pattern Recognition, 2006, pp. 728–735.
- [44] M. Donoser, M. Urschler, M. Hirzer, H. Bischof, Saliency driven total variation segmentation, in: Proceedings of the 12th IEEE International Conference on Computer Vision, 2009, pp. 817–824.
- [45] S. Mallat, *A Wavelet Tour of Signal Processing*, Academic Press, 1999.
- [46] W. Förstner, B. Moonen, A metric for covariance matrices, *Quo Vadis Geodesia*, 113–128.
- [47] J. Van De Weijer, T. Gevers, A.D. Bagdanov, Boosting color saliency in image feature detection, *IEEE Trans. Pattern Anal. Mach. Intell.* 28 (2006) 150–156.
- [48] A. Toshev, J. Shi, K. Daniilidis, Image matching via saliency region correspondences, in: Proceedings of the IEEE Conference on Computer Vision and Pattern Recognition, 2007, pp. 1–8.
- [49] Y. Sugano, Y. Matsushita, Y. Sato, Calibration-free gaze sensing using saliency maps, in: Proceedings of the IEEE Conference on Computer Vision and Pattern Recognition, 2010, pp. 2667–2674.
- [50] C.-Y. Lee, J.-J. Leou, H.-H. Hsiao, Saliency-directed color image segmentation using modified particle swarm optimization, *Signal Process.* 92 (2012) 1–18.

- [51] S. Feng, D. Xu, X. Yang, Attention-driven salient edges and regions extraction with application to CBIR, *Signal Process.* 90 (2010) 1–15.
- [52] H. Liu, F. Zhao, L. Jiao, Fuzzy spectral clustering with robust spatial information for image segmentation, *Appl. Soft Comput.* 12 (2012) 3636–3647.
- [53] F. Zhao, H. Liu, L. Jiao, Spectral clustering with fuzzy similarity measure, *Digital Signal Process.* 21 (2011) 701–709.
- [54] Y. Li, H. Shi, L. Jiao, R. Liu, Quantum evolutionary clustering algorithm based on watershed applied to SAR image segmentation, *Neurocomputing* 86(12) (2012) 90–98.
- [55] L. Jiao, Y. Li, M. Gong, X. Zhang, Quantum-inspired immune clonal algorithm for global optimization, *IEEE Trans. Syst., Man, Cybern. B* 38 (2008) 1234–1253.
- [56] P.K. Sahoo, G. Arora, Image thresholding using two-dimensional Tsallis Havrdá Charvát entropy, *Pattern Recognition Lett.* 27 (2006) 520–528.
- [57] D. Martin, C. Fowlkes, D. Tal, J. Malik, A database of human segmented natural images and its application to evaluating segmentation algorithms and measuring ecological statistics, in: *Proceedings of the IEEE International Conference on Computer Vision*, 2001, pp. 416–423.
- [58] (<http://cg.cs.tsinghua.edu.cn/people/~cmm/Saliency/Index.htm>).
- [59] (http://cns.bu.edu/~lgrady/random_walker_matlab_code.zip).
- [60] C. Pantofaru, M. Hebert, A comparison of image segmentation algorithms, *Robotics Institute*, 2005, pp. 336.
- [61] M. Meilă, Comparing clusterings: an axiomatic view, in: *Proceedings of the 22nd ACM International Conference on Machine Learning*, 2005, pp. 577–584.
- [62] J. Freixenet, X. Muñoz, D. Raba, J. Martí, X. Cufi, Yet another survey on image segmentation: region and boundary information integration, *Proceedings of the European Conference on Computer Vision (ECCV '02)*, Springer (2002) 408–422.
- [63] (http://www.eecs.berkeley.edu/~yang/software/lossy_segmentation/SegmentationBenchmark.zip).



Yicong Zhou received his B.S. Degree from Hunan University, Changsha, China, and his M.S. and Ph.D. Degrees from Tufts University, Massachusetts, USA, all degrees in Electrical Engineering. He is currently an Assistant Professor in the Department of Computer and Information Science at University of Macau, Macau, China. His research interests focus on Multimedia Security, Image/Signal Processing, Pattern Recognition and Medical Imaging. Dr. Zhou is a member of the IEEE and International Society for Photo-Optical Instrumentations Engineers (SPIE).



Wenbing Tao received his Ph.D. Degree in Pattern Recognition and Intelligent System from the Huazhong University of Science and Technology (HUST), Wuhan, China, in 2004. From 2005 to 2010, he had been with the School of Computer Science and Technology, HUST, where he was an Associate Professor. Since 2011, he moved to Institute for Pattern Recognition and Artificial Intelligence, HUST. He is a Research Fellow in Division of Mathematical Sciences, Nanyang Technology University from March 2008 to March 2009. His research interests lie in the area of Computer Vision, Image Segmentation, Object Recognition and Tracking. He has published numerous papers and conference papers in the area of image processing and object recognition. He serves as Reviewer for many journals, such as *International Journal of Computer Vision*, *IEEE Transactions on Image Processing*, *Pattern Recognition*, and so on.



Chanchan Qin was born in Shanxi, China, on October 4, 1983. She received the M.S. Degree in Physical Science and Technology from the Central China Normal University (CCNU), Wuhan, China, in 2010. She is currently pursuing the Ph.D. Degree in Physical Science and Technology from Central China Normal University (CCNU), Wuhan, China. Her research interests include Computer Vision, Image Segmentation, and Pattern Recognition.



Guoping Zhang received his Ph.D. Degree in Electronic Information from the Huazhong University of Science and Technology (HUST), Wuhan, China, in 1995. Since 1998, he has been with the College of Physical Science and Technology at Central China Normal University (CCNU), where he is currently a Professor. His research interests lie in the area of Computer Vision, Signal Processing and Photoelectric Information Technology.

Zhiguo Cao received his Ph.D. Degree in Pattern Recognition and Intelligence Systems in 2001 from Huazhong University of Science and Technology, Wuhan, China, where he is currently a Professor. His research interests are Pattern Recognition, Image Processing, and Data Fusion.